

**Enhancement of circularly polarized electroluminescence via reflection reversal under a magnetic field**

Journal:	<i>Journal of Materials Chemistry C</i>
Manuscript ID	TC-ART-01-2024-000048.R1
Article Type:	Paper
Date Submitted by the Author:	02-Feb-2024
Complete List of Authors:	Suzuki, Seika; Kindai University, Applied Chemistry, Faculty of Science and Engineering Yamamoto, Yuta; Kindai University Faculty of Science and Engineering Graduate School of Science and Engineering, Kitahara, Maho; Kindai University Shikura, Ryuta; Osaka Metropolitan University, Graduate School of Engineering Yagi, Shigeyuki ; Osaka Metropolitan University Department of Engineering Graduate School of Engineering Imai, Yoshitane; Kindai University, Department of Applied Chemistry

ARTICLE

Enhancement of circularly polarized electroluminescence via reflection reversal under a magnetic field

Seika Suzuki,^a Yuta Yamamoto,^a Maho Kitahara,^a Ryuta Shikura,^b Shigeyuki Yagi,^b Yoshitane Imai^{*a}

Received 00th January 20xx,
Accepted 00th January 20xx

DOI: 10.1039/x0xx00000x

Electroluminescent devices such as circularly polarised organic light-emitting diodes (CP-OLEDs) fabricated by conventional methods do not exhibit adequate circularly polarised electroluminescence (CPEL) with high circular polarisation. Therefore, new approaches for CPEL and CP-OLED systems are needed. We developed an external-magnetic-field-driven CP-OLED device that emits red CPEL by integrating an achiral optically inactive phosphorescent platinum(II) porphyrin luminophore (PtOEP) in the emission layer (EML). This magnetic CP-OLED system can simultaneously emit circularly polarised light with opposite rotations from the EML in the N-up and S-up directions of the applied magnetic field. By utilising this mechanism that allows simultaneous emission upon the application of a magnetic field and the reflection-reversal property of circularly polarized light, we may suppress the decrease in both the luminosity and circular polarisation of CPEL. The direction of rotation of CPEL was successfully reversed by switching the Faraday geometry of the applied magnetic field. This approach can promote the development of novel CP-OLED devices.

Introduction

In recent years, several optically active chiral luminophores with large anisotropy coefficients (g_{CPL}) as well as high photoluminescence quantum yields (Φ_{PL}) have been extensively used in the emitting layers of devices exhibiting circularly polarised electroluminescence (CPEL).¹⁻⁴

Several phosphorescent Pt(II) luminophores bearing organic ligands have been reported in recent years.⁵⁻¹⁰ In particular, phosphorescent organic Pt(II) luminophores with bidentate, tridentate, and tetradentate organic ligands have shown potential as a constituent of emitting layers (EMLs) in devices exhibiting electroluminescence (EL).¹¹⁻¹⁷ This is attributed to the fact that Pt(II) luminophores emit phosphorescence with a high quantum yield (Φ_{PL}) owing to strong spin-orbit interactions. Furthermore, Pt(II) luminophores have been reported to emit circularly polarised luminescence (CPL) when incorporated with chiral substituents or chiral auxiliaries as ligands although their structural framework is basically achiral owing to their square planar coordination geometry.¹⁸⁻²⁵ Moreover, they possess a narrow CPL bandwidth in the visible region and high g_{CPL} values, which will result in high-performance CPEL.²⁶⁻²⁹

However, preparing optically isomeric luminophores with high enantiomeric purity in a short time and at a low cost by

current methods is difficult. Thus, the exploration of new approaches for the development of CPEL and circularly polarised organic light-emitting diode (CP-OLED) systems is necessitated.

In recent years, external static magnetic fields have garnered significant attention as a physical bias to induce circularly polarised signals in the photoexcited states of achiral and racemic organic, organic-inorganic, or inorganic luminescent materials.³⁰⁻⁴⁵ In this context, we have succeeded in generating full-colour red-green-blue-yellow (RGBY) CPEL under a magnetic field from organic light-emitting diodes (OLEDs) incorporated with optically inactive phosphorescent iridium(III) luminophores in the EML. That is, the application of an external magnetic field allows us to develop phosphorescent CP-OLEDs without any chiral phosphors, namely, magnetic CP-OLED (MCP-OLEDs).⁴⁶ We also reported that OLEDs with varying concentrations of an excimer-emissive heteroleptic cyclometalated Pt(II) complex as an emitting dopant exhibit multi-colour magnetically induced CPEL (MCPEL). At lower doping levels of the Pt(II) luminophore in the EML, monomer-based emission-enriched bluish CPEL was observed from the devices upon the application of a magnetic field. When the doping level increased, the excimer-based CPEL was superior to the monomer-based one, and finally excimer-based orange CPEL was exclusively observed.⁴⁷

In this work, we prepare novel OLEDs that exhibits MCPEL, which comprises an optically inactive porphyrin-based platinum(II) luminophore, namely, 2,3,7,8,12,13,17,18-octaethylporphyrinato)platinum(II) (PtOEP, Figure 1). When PtOEP is doped into the EML of the OLED, highly efficient red MCPEL is observed. Furthermore, this MCP-OLED system can control the rotation direction of red MCPEL on the basis of the direction of the applied magnetic field. In conventional and

^a Graduate School of Science and Engineering, Kindai University, 3-4-1 Kowakae, Higashi-Osaka, Osaka 577-8502, Japan.

^b Department of Applied Chemistry, Graduate School of Engineering, Osaka Metropolitan University, 1-1 Gakuen-cho, Naka-ku, Sakai, Osaka 599-8531, Japan.

Electronic Supplementary Information (ESI) available: Photographs of EL, EL spectra at various voltages, current efficiency profiles, and EQE profiles of the MCP-OLED devices. See DOI: 10.1039/x0xx00000x

generic CP-OLED systems, CPL reflected from the cathode interferes with CPL emitted from the indium tin oxide (ITO) electrode. In other words, the rotation of the directly extracted circularly polarised light is cancelled out by the sign-inverted, reflected CPL. Here, we propose new mechanism of external-magnetic-field-driven Pt-based OLEDs, where CPEL with high brightness and at a high anisotropic rate is extracted from the device under an external magnetic field, with an assist of the reflection reversal of circularly polarized light.

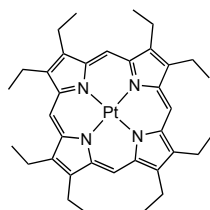


Figure 1. Achiral Pt(II) luminophore PtOEP.

Experimental

Materials

PtOEP was purchased from Sigma-Aldrich, Japan (Tokyo, Japan). Pre-patterned ITO substrates were prepared by depositing ITO on alkali-free glass.

Fabrication of magnetic circularly polarised electroluminescence (MCPEL) devices

ITO-glass substrates (ITO thickness, 50 nm; sheet resistance, 50 Ω /sq) were purchased from GEOMATEC Co., Ltd. The ITO-coated glass substrates were ultrasonically cleaned in a solution containing ultra-pure water and an alkaline detergent solution. The surfaces were treated with isopropyl alcohol vapour followed by ultraviolet–ozone treatment. Subsequently, all organic thin films and Al (or Mg/Ag) were deposited through vacuum evaporation. During deposition, the temperature of the evaporation source was monitored, and the doping concentration of the EML was adjusted by the precise control of

the deposition rate. The deposition system was connected to a glove box (concentrations of oxygen and moisture < 10 ppm) through a load lock chamber. Therein, after the deposition procedures, the devices were sealed in a glass can to keep them from air and moisture. Four devices were fabricated on each substrate.

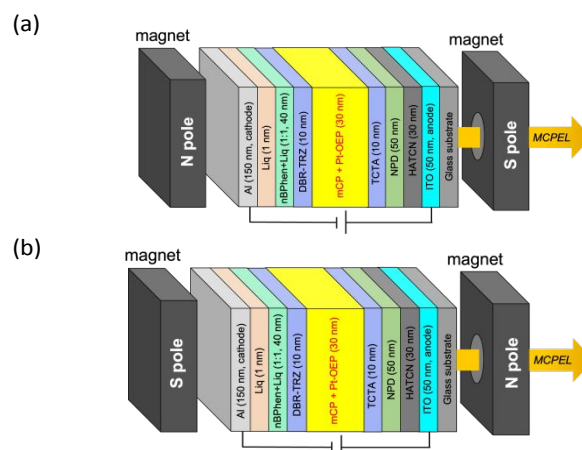
Measurement of EL, magnetic electroluminescence (MEL), and MCPEL

The brightness of outcoupled emission from the fabricated devices was recorded using a BM-9 luminance meter (TOPCON TECHNOHOUSE CORPORATION, Japan). The OLED performance of the fabricated device was evaluated at 25 °C using a Hamamatsu Photonics C-9920-11 organic EL device evaluating system (Hamamatsu, Japan).

The MCPEL and unpolarised MEL spectra of the MCP-OLEDs were acquired at 25 °C using a JASCO CPL-300 spectrofluoropolarimeter (Hachioji, Tokyo, Japan). A 1.7-T external magnetic field was applied using a JASCO PM-491 permanent magnet (Hachioji, Tokyo, Japan). The emission bandwidth was 10 nm.

Results and discussion

Two types of MCP-OLEDs [Al/ITO-Device-I and MgAg/ITO-Device-II (or ITO/MgAg-Device-II)] containing PtOEP as the emitting dopant were fabricated using a non-transparent, mirror-like Al or light-transmissive MgAg alloy as the cathode electrode. The structure of these devices (shown in Figure 2) is as follows:⁴⁸ ITO (anode, 50 nm) / 1,4,5,8,9,11-hexaazatriphenylenehexacarbonitrile (HATCN, 30 nm) / *N,N'*-di-1-naphthyl-*N,N'*-diphenylbenzidine (NPD, 50 nm) / 4,4',4''-tris(carbazol-9-yl)triphenylamine (TCTA, 10 nm) / EML (30 nm) / 2-[3'-(dibenzothiophen-4-yl)-1,1'-biphenyl-3-yl]-4,6-diphenyl-1,3,5-triazine (DBT-TRZ, 10 nm) / 2,9-dinaphthalen-2-yl-4,7-diphenyl-1,10-phenanthroline:8-hydroxyquinolinolato-lithium (nBphen : Liq, 40 nm) / Liq (1 nm) / Al (cathode, 150 nm) or MgAg (9/1 wt/wt) (cathode, 10 nm), where the EML consisted of 1,3-di(9*H*-carbazol-9-yl)benzene (mCP) and PtOEP (84/16 wt/wt).



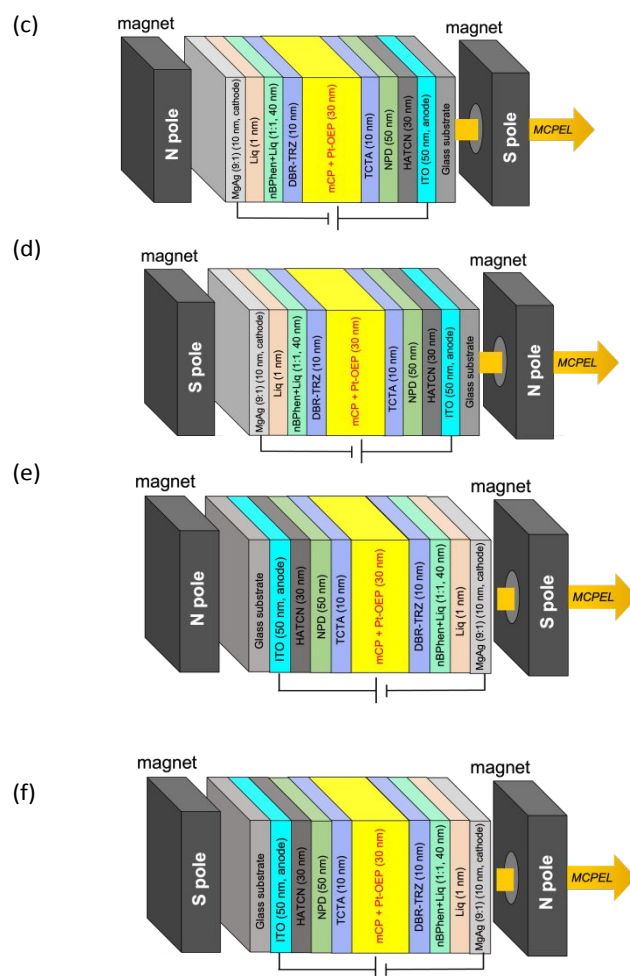


Figure 2. Magnetic circularly polarised electroluminescence (MCPEL) system with magnetic N and S poles. (a) NS-Al/ITO-Device-I, (b) SN-Al/ITO-Device-I, (c) NS-MgAg/ITO-Device-II, (d) SN-MgAg/ITO-Device-II, (e) NS-ITO/MgAg-Device-II, and (f) SN-ITO/MgAg-Device-II

First, using these three types of devices, we examined whether devices doped with the optically inactive porphyrin-based platinum(II) emitter (PtOEP) could operate as high-performance OLEDs, i.e., whether the surfaces of these three devices can exhibit EL of sufficient brightness.

The emission colour and EL characteristics of the resulting MCP-OLED devices were evaluated. The voltage was fixed at 13 V, and the emission colour coordinate and EL spectra were measured for each device.

Photograph of the emitting devices and EL spectra are shown in Figures S1 and 3(a), respectively. In addition, the EL spectra measured at various applied voltages are shown in Figure S2. The maximum EL wavelengths (λ_{EL}) and observed EL characteristics of the three device configurations (Al/ITO-Device I, MgAg/ITO-Device II, and ITO/MgAg-Device II) are summarised in Table 1. Each MCP-OLED device exhibited clear red EL at approximately 650 nm upon voltage application. The Commission Internationale de l'Eclairage (CIE) chromaticity coordinates (CIE (x, y)) of (0.63, 0.29), (0.62, 0.27), and (0.63,

0.28) were achieved for Al/ITO-Device I, MgAg/ITO-Device II, and ITO/MgAg-Device II, respectively, at the maximum luminance (L_{max}). In general, the EL spectrum of the OLED device is almost similar to the PL spectrum of the corresponding emitting material. This phenomenon was also observed for Devices I and II with PtOEP. These colour coordinates are approximately close to the National Television System Committee (NTSC) standard of red, CIE (0.67, 0.33). This indicates that the difference in the cathode electrode does not have any significant impact on the EL characteristics, such as the EL wavelength and the CIE chromaticity coordinate. Moreover, even when the electroluminescence was extracted from the cathode of Device II (i.e., ITO/MgAg-Device II), the EL spectrum and CIE coordinate of the observed EL were identical to those of Al/ITO-Device I and MgAg/ITO-Device II.

Furthermore, the EL characteristics of the MCP-OLED device were evaluated. The voltage was fixed at 13 V and the current density was measured. The luminance–voltage–current density, current efficiency–current density, and external quantum efficiency (EQE)–current density profiles are shown in Figures 3,

S3, and S4, respectively. The emission intensity of Device I, equipped with non-transparent Al as the cathode, was significantly higher than that of Device II, which used transparent MgAg as the cathode (Table 1). MCP-OLED Device I, equipped with non-transparent Al as the cathode, exhibited much more intense EL than Device 2 having transparent MgAg as the cathode, affording an L_{\max} of 554.8 cd/m^2 at 13 V. This is because light from the EML to the cathode is reflected from mirror-like Al in Device I, resulting in a higher intensity of light outcoupled from the ITO side (Table 1, Al/ITO-Device I). In contrast, in MCP-OLED Device II, the light from the EML to the cathode passes through transmissive MgAg; thus, the intensity of light outcoupled from ITO and MgAg is low (Table 1, MgAg/ITO-Device II and ITO/MgAg-Device II). Device II with the MgAg cathode electrode exhibited a L_{\max} of 55.5 cd/m^2 at 13 V from the ITO electrode side and 63.5 cd/m^2 from the MgAg electrode side. As expected, the L_{\max} of Device I with the Al electrode was approximately 10 times higher than that of Device II with the Mg/Ag electrode. From the results above, the present system of PtOEP-containing MCP-OLED devices is useful to investigate CPEL behaviour outcoupled from both of the cathode and anode.

In addition, a slight decrease in the maximum current efficiency $\eta_{j, \max}$ was observed when the cathode electrode was changed from the Al to MgAg material. In particular, the EQE was higher for Device I with the Al material. This suggests the following points: (1) the Al material is more suitable as the cathode to obtain high device performance, (2) the EL properties of these devices are primarily derived from PtOEP, and (3) charge carrier injection to the EML is efficient to induce intense EL from PtOEP.

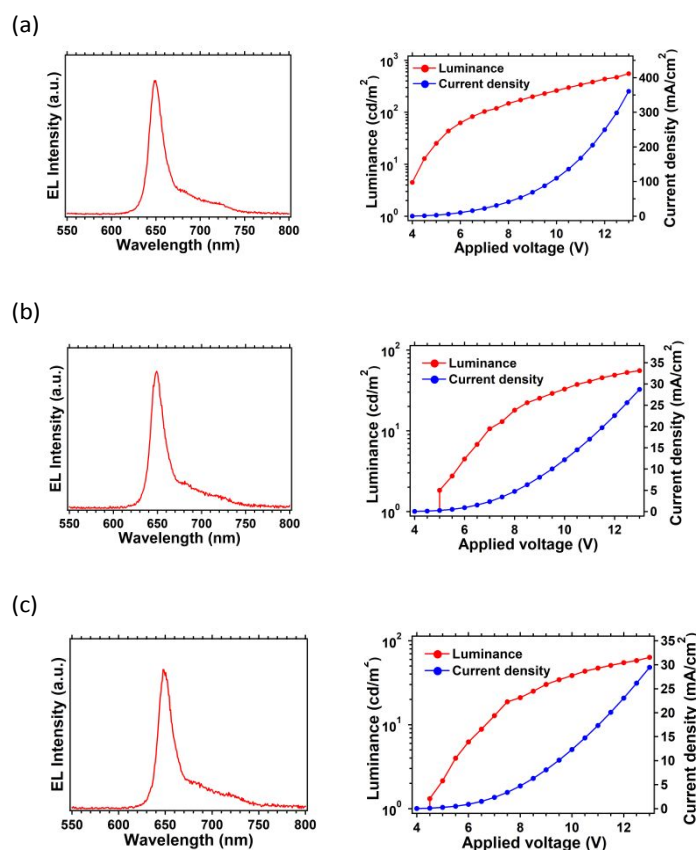


Figure 3. EL spectra (left) at 13 V and luminance–voltage–current density profiles (right) for (a) Al/ITO-Device I, (b) MgAg/ITO-Device II, and (c) ITO/MgAg-Device II.

Table 1. EL characteristics of Al/ITO-Device I, MgAg/ITO-Device II, and ITO/MgAg-Device II.

Device	Al/ITO-Device I	MgAg/ITO-Device II	ITO/MgAg-Device II
λ_{EL} (nm)	649	650	650
$V_{\text{on}}^{\text{[a]}}$ (V)	3.5	5.0	4.5
$L_{\max}^{\text{[b]}}$ (cd m^{-2})	554.8	55.5	63.5
[@V]	[13.0]	[13.0]	[13.0]
$\eta_{j, \max}^{\text{[b]}}$ (cd A^{-1})	1.35	0.69	1.13
[@V]	[3.5]	[5.0]	[4.5]
CIE (x, y) ^[c]	(0.63, 0.29)	(0.62, 0.27)	(0.63, 0.28)
EQE	2.75 [4.5]	1.74 [5.0]	2.25 [5.5]

^[a] Turn-on voltages at which luminance of $>1 \text{ cd/m}^2$ was achieved. ^[b] Maximum values of luminance (L) and current efficiency (η_j). The voltages in parentheses are those at which they were obtained. ^[c] Commission Internationale de l'Eclairage chromaticity coordinates.

The MCP-EL properties of these MCP-OLED devices were studied at 25 °C under a 1.7-T magnetic field. For the MCP-EL and MEL analysis, the applied voltage was fixed at 13 V for all devices. The MCP-EL and MEL spectra of the obtained devices are shown in Figure 4, and the MCP-EL properties are summarised in Table 2. Red MCP-EL was detected from all three directions: from the ITO side of Device I (Figures 2a and 2b) and from the ITO (Figures 2c and 2d) and MgAg (Figure 2e and 2f) sides of Device II. As expected, for each device, the sign of the MCP-EL spectrum could be completely controlled by changing the arrangement of the N and S magnets. In other words, mirror-symmetric MCP-EL spectra were obtained by alternating the arrangement of the N-up and S-up Faraday geometries.

In all the fabricated MCP-OLED devices, the MCP-EL spectra in the N-up geometry were negatively signed (red line spectra in Figures 4a–c) and those in the S-up geometry were positively signed (blue line spectra in Figures 4a–c), regardless of emission from the ITO or MgAg side. The MCP-EL and MEL spectra of these devices were similar to the magnetically induced CPL (MCPL) and magnetically induced PL spectra of PtOEP that was doped on polymethyl methacrylate (PMMA) films.²⁹ The trend of the chiroptical signature for MCP-EL of the as-prepared devices is the same as that observed for MCPL of PtOEP for the same Faraday configuration in a dichloromethane (CH_2Cl_2) solution and PMMA film.

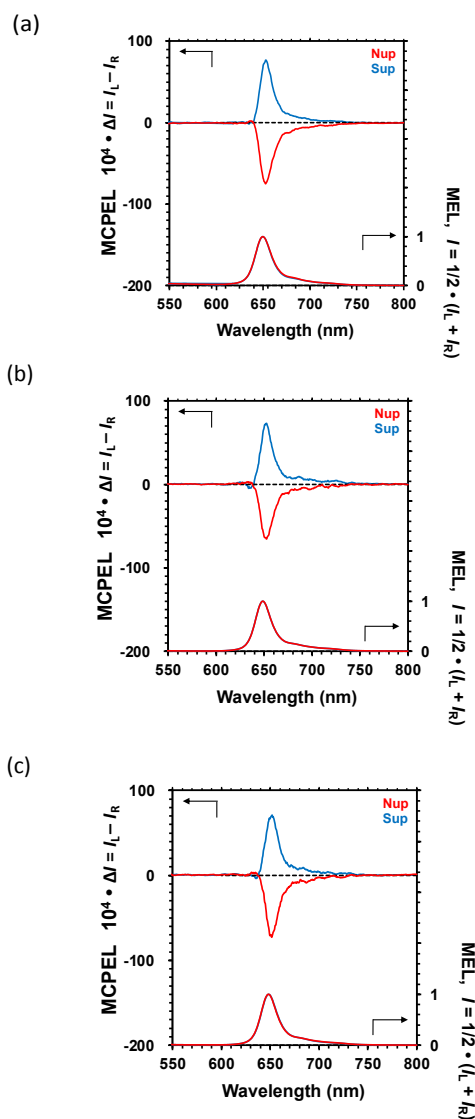


Figure 4. MCPEL (upper panel) and MEL (lower panel) spectra for (a) NS- and SN-Al/ITO-Device I, (b) NS- and SN-MgAg/ITO-Device II, and (c) NS- and SN-ITO/MgAg-Device II under 1.7 T N-up (red lines) and S-up (blue lines) magnetic fields.

Table 2. MCPEL characteristics of (a) NS-Al/ITO-Device I, (b) SN-Al/ITO-Device I, (c) NS-MgAg/ITO-Device II, (d) SN-MgAg/ITO-Device II, (e) NS-ITO/MgAg-Device II, and (f) SN-ITO/MgAg-Device II under a 1.7-T magnetic field.

Device	λ_{MCPEL} (nm)	$ g_{\text{MCPEL}} / \times 10^{-3} (\text{T}^{-1})$	MCPEL sign
NS-Al/ITO-Device-I	653	7.9	(-)
SN-Al/ITO-Device-I	653	8.3	(+)
NS-MgAg/ITO-Device-II	653	7.3	(-)
SN-MgAg/ITO-Device-II	653	8.2	(+)
NS-ITO/MgAg-Device-II	652	7.9	(-)
SN-ITO/MgAg-Device-II	652	7.8	(+)

Furthermore, the performance of the MCP-OLED devices was quantitatively evaluated using the dissymmetry factor ($g_{\text{MCPEL}} = (I_L - I_R) / [1/2(I_L + I_R)]$, where I_L and I_R are the amplitude intensities of the left- and right-handed MCPEL, respectively). The MCPEL efficiency, $|g_{\text{MCPEL}}|$, of Device I was 7.9×10^{-3} for N-up and 8.3×10^{-3} for S-up. These results indicate that red MCPEL can be efficiently emitted under an external magnetic field of 1.7 T by using an EL device containing optically inactive Pt(II) luminophore. Conversely, the $|g_{\text{MCPEL}}|$ of MCP-OLED Device II was 7.3×10^{-3} for N-up and 8.2×10^{-3} for S-up from ITO. The $|g_{\text{MCPEL}}|$ of MCP-OLED Device II is 7.9×10^{-3} for N-up and 7.8×10^{-3} for S-up from MgAg. These $|g_{\text{MCPEL}}|$ values were on the same order ($7\text{--}8 \times 10^{-3}$), showing negligible differences. Moreover, they were nearly identical to the absolute values for the dissymmetry factor of MCPL (g_{MCPL}) of PtOEP in toluene (6.1×10^{-3} at 646 nm) and in the PMMA film (8.9×10^{-3} at 648 nm).⁵⁰

In the case of CP-OLED devices employing chiral luminophores, deterioration of dissymmetry factor (g -factor) of CPEL is often reduced unfavourably, due to several potential causes including interference of circular polarisation at multiple interfaces of the multilayer device and the rotational direction of reflection reversal of light by the non-transparent metal cathode.⁵⁰⁻⁵² Interestingly, the $|g_{\text{MCPEL}}|$ values of MCPEL from Device I are similar to the $|g_{\text{MCPL}}|$ values of PtOEP, showing no remarkable decrease. This confirms that MCP-OLED devices are less affected by the unfavourable factors to reduce g_{MCPEL} . In Device I, CPEL with opposite rotational directions is emitted from the EML containing PtOEP in both the N-up and S-up directions, as shown in Figure 5.

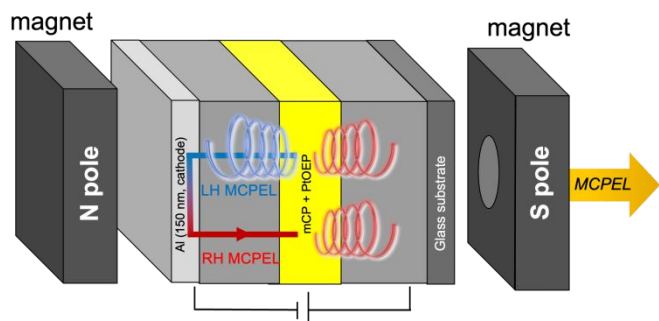


Figure 5. MCPEL system with magnetic N and S poles. LH and RH MCPEL indicate left- and right-handed MCPEL, respectively.

Thus, CPEL in the S-up direction is reflected and reversed at the mirror-like Al electrode. This sign-inverted CPEL is in the same direction of rotation as that of directly outcoupled CPEL in the N-up direction. Thus, there is no decrease in the g-factor of CPEL from the device. This is confirmed from the fact that the signs of the CPEL spectra in configurations (a) and (f) in Figure 2 (or configurations (b) and (e) in Figure 2) are opposite to each other. In other words, the CPEL spectrum in the S-up direction in configuration (a) in Figure 2 is equivalent to that in the S-up direction in configuration (f) in Figure 2. Similarly, the CPEL spectrum in the N-up direction in configuration (b) in Figure 2 represents that in the N-up direction in configuration (e) in Figure 2. That is, we demonstrated the difference in CPEL outcoupling between CP-OLED and MCP-OLED devices: the MCP-OLED device allowed the extraction of CPEL with enhanced efficiency in relation to the CP-OLED device.

These results confirm that the application of an external magnetic field can not only switch the rotational direction of generated CPEL but also improve both the g-factor and luminosity of CPL. We believe that this study is a breakthrough in the development of magnetic-field-based, highly functional CPEL systems.

Conclusions

We developed external-magnetic-field-driven CP-OLEDs containing an achiral phosphorescent Pt(II) porphyrin luminophore in the EML, which emit red CPEL. In all the fabricated devices, the chiroptical signature for MCPEL was controlled according to the Faraday geometry of the magnetic field. Interestingly, when the EL properties were compared between the single-sided and double-sided transmissive devices, the EL intensity (i.e., L_{\max}) of the single-sided transmissive device was approximately 10 times larger than

that of the double-sided transmissive device. Moreover, the single-sided transmissive device showed a g-factor of MCPEL that is comparable to that of the double-sided transmissive device. This indicates that CP-OLED devices can amplify both the degree of light rotation and luminance under an external magnetic field, by capitalising on the light reflection reversal. These findings will promote the exploration of new approaches toward the development of CPL materials and CP-OLED devices.

Author Contributions

This work was conceived by Yoshitane Imai, who also supervised all experiments and drafted the manuscript. Seka Suzuki, Yuta Yamamoto, Maho Kitahara, and Ryuta Shikura recorded the spectra and evaluated the obtained spectra. Shigeyuki Yagi and Yoshitane Imai provided constructive guidance for this study.

Conflicts of interest

There are no conflicts to declare.

Acknowledgements

This research was supported by JST-CREST (JPMJCR2001), JST-A-STEP (JPMJTM22D9), Grants-in-Aid for Scientific Research (KAKENHI JP21K18940 and JP23H02040) from the MEXT/Japan Society for the Promotion of Science, and grants from the Takahashi Industrial and Economic Research Foundation (2020), Research Foundation for Opto-Science and Technology (2020-5), Ichimura Foundation for New Technology (2020-04), and SCAT Foundation (2021).

References

- [1] U. V. Valiev, J. B. Gruber, G. W. Burdick, A. K. Mukhammadiev, D. Fu and V. O. Pelenovich, *J. Lumin.*, 2014, **145**, 393–401.
- [2] F. Zinna, M. Pasini, F. Galeotti, C. Botta, L. D. Bari and U. Giovannella, *Adv. Funct. Mater.*, 2017, **27**, 1603719.
- [3] M. Li, S. H. Li, D. Zhang, M. Cai, L. Duan, M. K. Fung and C. F. Chen, *Angew. Chem. Int. Ed.*, 2018, **57**, 2889–2893.
- [4] L. Frédéric, A. Desmarchelier, R. Plais, L. Lavnech, G. Muller, C. Villafuerte, G. Clavier, E. Quesnel, B. Racine, S. Meunier-Della-Gatta, J. P. Dognon, P. Thuéry, J. Crassous, L. Favereau and G. Pieters, *Adv. Funct. Mater.*, 2020, **30**, 2004838.
- [5] D. R. McMillin and J. J. Moore, *Coord. Chem. Rev.*, 2002, **229**, 113–121.
- [6] J. Brooks, Y. Babayan, S. Lamansky, P. I. Djurovich, I. Tsyba, R. Bau and M. E. Thompson, *Inorg. Chem.*, 2002, **41**, 3055–3066.
- [7] T. J. Wadas, Q. M. Wang, Y. J. Kim, C. Flaschenreim, T. N. Blanton and R. Eisenberg, *J. Am. Chem. Soc.*, 2004, **126**, 16841–16849.
- [8] Y. D. Chen, Y. H. Qin, L. Y. Zhang, L. X. Shi and Z. N. Chen, *Inorg. Chem.*, 2004, **43**, 1197–1205.
- [9] B. C. Tzeng, T. H. Chiu, S. Y. Lin, C. M. Yang, T. Y. Chang, C. H. Huang, A. H. H. Chang and G. H. Lee, *Cryst. Growth Des.*, 2009, **9**, 5356–5362.
- [10] A. Martín, Ú. Belío, S. Fuertes and V. Sicilia, *Eur. J. Inorg. Chem.*, 2013, 2231–2247.
- [11] H. Fukagawa, T. Shimizu, H. Hanashima, Y. Osada, M. Suzuki and H. Fujikake, *Adv. Mater.*, 2012, **24**, 5099–5103.

- [12] T. Fleetham, G. Li, L. Wen and J. Li, *Adv. Mater.*, 2014, **26**, 7116–7121.
- [13] H. Leopold, U. Heinemeyer, G. Wagenblast, I. Münster and T. Strassner, *Chem. Eur. J.*, 2017, **23**, 1118–1128.
- [14] T. Fleetham, G. Li and J. Li, *Adv. Mater.*, 2017, **29**, 1601861.
- [15] N. Okamura, T. Maeda, H. Fujiwara, A. Soman, K. N. N. Unni, A. Ajayaghosh and S. Yagi, *Phys. Chem. Chem. Phys.*, 2018, **20**, 542–552.
- [16] N. Okamura, K. Egawa, T. Maeda and S. Yagi, *New J. Chem.*, 2018, **42**, 11583–11592.
- [17] T. Maganti and K. Venkatesan, *ChemPlusChem*, 2022, **87**, e202200014.
- [18] T. Ikeda, M. Takayama, J. Kumar, T. Kawai, and T. Haino, *Dalton Trans.*, 2015, **44**, 13156–13162.
- [19] N. Saleh, B. Moore II, M. Srebro, N. Vanthuyne, L. T. Toupet, J. A. G. Williams, C. Roussel, K. K. Deol, G. Muller, J. Autschbach and J. Crassous, *Chem. Eur. J.*, 2015, **21**, 1673–1681.
- [20] X. P. Zhang, V. Y. Chang, J. Liu, X. L. Yang, W. Huang, Y. Li, C. H. Li, G. Muller and X. Z. You, *Inorg. Chem.*, 2015, **54**, 143–152.
- [21] S. Tanaka, K. Sato, K. Ichida, T. Abe, T. Tsubomura, T. Suzuki and K. Shinozaki, *Chem. Asian J.*, 2016, **11**, 265–273.
- [22] J. Song, M. Wang, X. Zhou and H. Xiang, *Chem. Eur. J.*, 2018, **24**, 7128–7132.
- [23] G. Park, H. Kim, H. Yang, K. R. Park, I. Song, J. H. Oh, C. Kim and Y. You, *Chem. Sci.*, 2019, **10**, 1294–1301.
- [24] J. Morikubo and T. Tsubomura, *Inorg. Chem.*, 2022, **61**, 17154–17165.
- [25] J. Han, Y. Wang, J. Wang, C. Wu, X. Zhang and X. Yin, *J. Organomet. Chem.*, 2022, **973-974**, 122394 (6 pages).
- [26] P. T. Chou and Y. Chi, *Chem. Eur. J.*, 2007, **13**, 380–395.
- [27] K. M. C. Wong, M. M. Y. Chan and V. W. W. Yam, *Adv. Mater.*, 2014, **26**, 5558–5568.
- [28] Z.-P. Yan, X.-F. Luo, W.-Q. Liu, Z.-G. Wu, X. Liang, K. Liao, Y. Wang, Y.-X. Zheng, L. Zhou, J.-L. Zuo, Y. Pan and H. Zhang, *Chem. Eur. J.*, 2019, **25**, 5672–5676.
- [29] K. Matsudaira, Y. Mimura, J. Hotei, S. Yagi, K-i. Yamashita, M. Fujiki and Y. Imai, *Chem. Asian J.*, 2021, **16**, 926–930.
- [30] K. E. Knowles, H. D. Nelson, T. B. Kilburn, and D. R. Gamelin, *J. Am. Chem. Soc.*, 2015, **137**, 13138–13147.
- [31] T. Wu, J. Kapitan, V. Andrushchenko and P. Bour, *Anal. Chem.*, 2017, **89**, 5043–5049.
- [32] E. L. Ivchenko, *Phys. Solid State*, 2018, **60**, 1514–1526.
- [33] S. Ghidinelli, S. Abbate, G. Mazzeo, L. Paoloni, E. Viola, C. Ercolani, M. P. Donzello and G. Longhi, *Chirality*, 2020, **32**, 808–816.
- [34] D. Kaji, H. Okada, N. Hara, Y. Kondo, S. Suzuki, M. Miyasaka, M. Fujiki and Y. Imai, *Chem. Lett.*, 2020, **49**, 674–676.
- [35] H. Yoshikawa, G. Nakajima, Y. Mimura, T. Kimoto, Y. Kondo, S. Suzuki, M. Fujiki and Y. Imai, *Dalton Trans.*, 2020, **49**, 9588–9594.
- [36] Y. Imai, *Symmetry*, 2020, **12**, 1786.
- [37] H. Okada, N. Hara, D. Kaji, M. Shizuma, M. Fujiki and Y. Imai, *Phys. Chem. Chem. Phys.*, 2020, **22**, 13862–13866.
- [38] T. Kimoto, Y. Mimura, M. Fujiki and Y. Imai, *Chem. Lett.*, 2021, **50**, 916–919.
- [39] K. Mishima, D. Kaji, M. Fujiki and Y. Imai, *ChemPhysChem*, 2021, **22**, 1728–1737.
- [40] Y. Mimura, M. Fujiki and Y. Imai, *Chem. Phys. Lett.*, 2021, **767**, 138353 (4 pages).
- [41] K. Matsudaira, A. Izumoto, Y. Mimura, Y. Kondo, S. Suzuki, S. Yagi, M. Fujiki and Y. Imai, *Phys. Chem. Chem. Phys.*, 2021, **23**, 5074–5078.
- [42] S. Ghidinelli, S. Abbate, G. Mazzeo, R. Paolesse, G. Pomarico and G. Longhi, *ACS Omega*, 2021, **6**, 26659–26671.
- [43] Y. Imai, *ChemPhotoChem*, 2021, **5**, 969–973.
- [44] F. Zinna and G. Pescitelli, *Eur. J. Org. Chem.*, 2023, **26**, e202300509.
- [45] M. Kitahara, S. Suzuki, K. Matsudaira, S. Yagi, M. Fujiki and Y. Imai, *ChemistrySelect*, 2021, **6**, 11182–11187.
- [46] M. Kitahara, K. Hara, S. Suzuki, H. Iwasaki, S. Yagi, and Y. Imai, *Org Electron.*, 2023, **119**, 106814.
- [47] Y. Imai, Y. Yamamoto, S. Suzuki, K. Hara, M. Kitahara and S. Yagi, *Org. Electron.*, 2023, **122**, 106893.
- [48] We named the MCP-OLED devices as (Faraday geometry)-[cathode (or anode)]/[anode (or cathode)]-Device I or II. The sequence [cathode (or anode)]/[anode (or cathode)] represents [the electrode on the far side of the detector]/[the electrode on the near side of the detector]. For the Faraday geometry, NS represents N and S poles on the far and near sides of the detector, respectively (N-up), and SN represents the opposite configuration (S-up).
- [49] E. Peeters, M. P. T. Christiaans, R. A. J. Janssen, H. F. M. Schoo, H. P. J. M. Dekkers and E. W. Meijer, *J. Am. Chem. Soc.*, 1997, **119**, 9909–9910.
- [50] F. Zinna, U. Giovanella and L. Di. Bari, *Adv. Mater.*, 2015, **27**, 1791-1975.
- [51] V. Adamovich, J. Brooks, A. Tamayo, A. M. Alexander, P. I. Djurovich, B. W. D'Andrade, C. Adachi, S. R. Forrest and M. E. Thompson, *New J. Chem.*, 2002, **26**, 1171–1178,
- [52] L. Frédéric, A. Desmarchelier, L. Favereau and G. Pieters, *Adv. Funct. Mater.*, 2021, **31**, 2010281.